Supplementary Informations

MgFeTi-LDH/g-C_3N_4 promote sodium persulfate activation through Fe^{3+}/Fe^{2+} cycle for efficient tetracycline degradation under visible light irradiation

Zihan Wei[a‡], Xiaoqian Ren[b‡], Tianhong Mei[a], Rongcheng Xiang[a], Wugan Wei[a], Xiaorui Yang[a], Yan Fang[a], Wenlong Xu[c], Jianliang Zhu[a], Jinhua Liang[a*]

[a] College of Biotechnology and Pharmaceutical Engineering, Nanjing Tech University, Nanjing, 211816, China

[b] College of Chemical Engineering, Nanjing Tech University, Nanjing, 211816, China

[c] Institute of Agricultural Resources and Environment, Jiangsu Academy of Agricultural Sciences, Nanjing, 210014, China

‡ These two authors contributed equally in composing it.

* Corresponding Authors: College of Biotechnology and Pharmaceutical Engineering, Nanjing Tech University, Nanjing, 211816, China.

E-mail address: jhliang@njtech.edu.cn (J. H. Liang).

Index

MgFeTi(3:1)-LDH/g-C_3N_4 at 30 min

Fig. S15 Optical density (OD_{600}) values of degradation TCH at different time periods over MgFeTi (3:1)-LDH/g-C_3N_4

Tab. S1 The specific surface areas, pore volumes, and pore sizes of catalyst

1. Radical-capturing experiment

A radical-capturing experiment is an effective approach to explain the reaction mechanism. Radical capturing agents were added during photocatalytic testing. chloroform (TCM, 10 mmol L^{-1}), ethylenediaminetetraacetic acid disodium salt (EDTA-2Na, 10 mmol L^{-1}), and methanol (MeOH, 10 mmol L^{-1}) were added as scavengers for superoxide radicals ($•O_2^-$), photo-generated holes (h^+), hydroxyl radicals (•OH).

2. Text toxicity assessment

Toxicity assessment is one of the key factors in evaluating the safety of wastewater treatment processes, particularly due to the potential formation of highly toxic intermediates during degradation. In order to determine the toxicity of TCH and intermediates, the toxicity estimation software tool (TEST) was applied to assess ecotoxicity according to various mathematical models of QSAR from Environmental Protection Agency database in US. Here，six toxicity parameters such as acute toxicity of fathead minnow (LC_{50}-96 h), daphnia magna 50% lethal dose (LC_{50}-48 h), oral rats (LD_{50}), bioconcentration factor, developmental toxicity, and mutagenicity are employed to evaluate the toxicity of TCH and degradation intermediates.

Furthermore, this work used OD_{600} value to evaluate toxicity of byproducts from TCH degradation. The degradation solution of 20 mg/L TCH was collected for bacterial culturing. *Escherichia coli* DH5α, a representative model bacterium, was selected to investigate its growth under the presence of TCH degradation solution. This experiment aims to assess the detoxification capacity of the system in treating TCH-contaminated wastewater, particularly focusing on

evaluating the potential of the degradation products to support bacterial growth without causing toxicity. In a typical run, the strain in logarithmic growth stage was inoculated in LB medium for toxicity test. The OD_{600} of *Escherichia coli DH5a* was measured to assess toxic inhibition after 24 h incubation at 25 ± 1 ℃. All experiments were repeated three times.

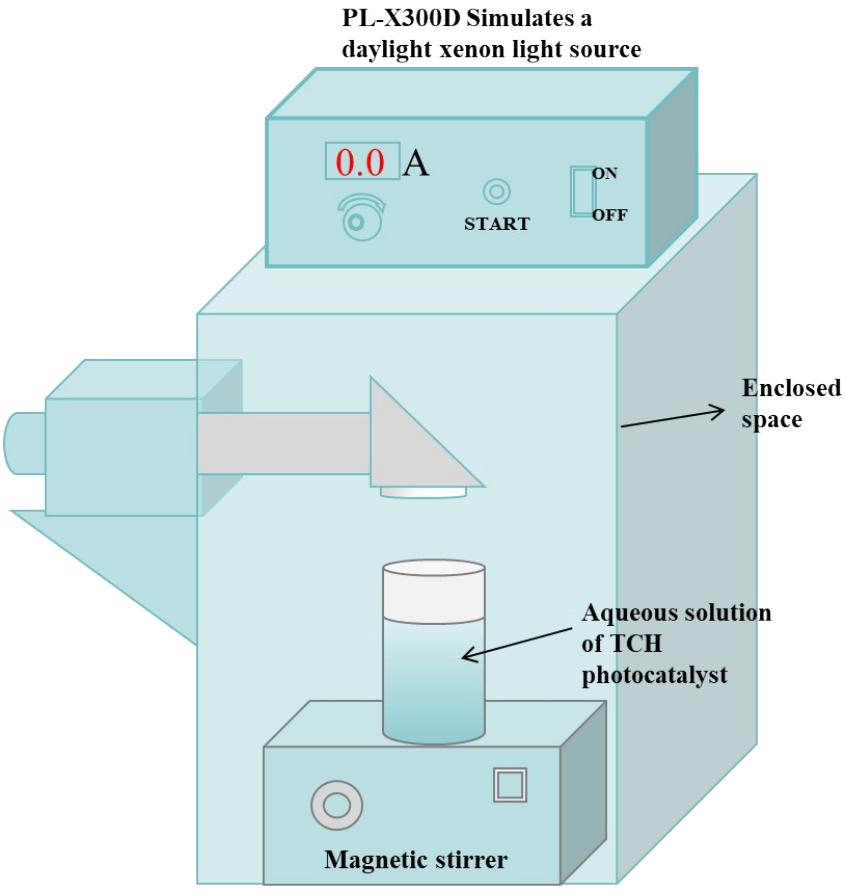

Fig. S1. Photocatalytic reaction device

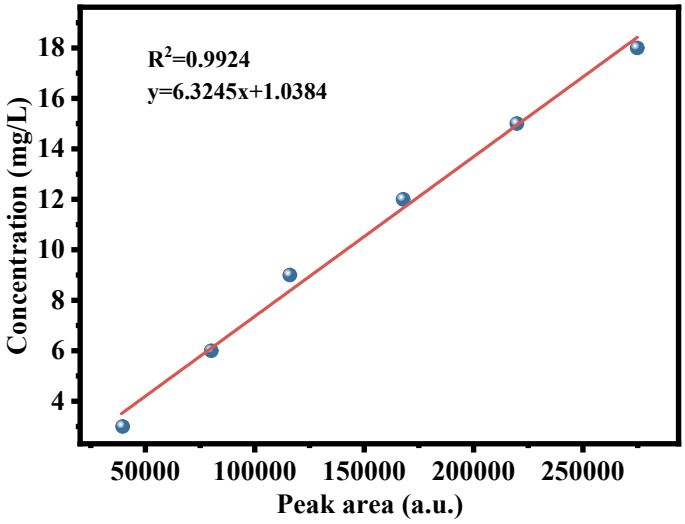

Fig. S2. Standard curve of TCH

Table S1 The specific surface areas, pore volumes, and pore sizes of catalyst

Sample	Specific surface area(m^2/g)	Pore volume(cm^3/g)	Pore size (nm)
g-C_3N_4	53.8	0.16	16.7
MgFeTi(3:1)-LDH	99.1	0.08	5.2
MgFeTi(3:1)-LDH/g-C_3N_4	83.2	0.42	13.6

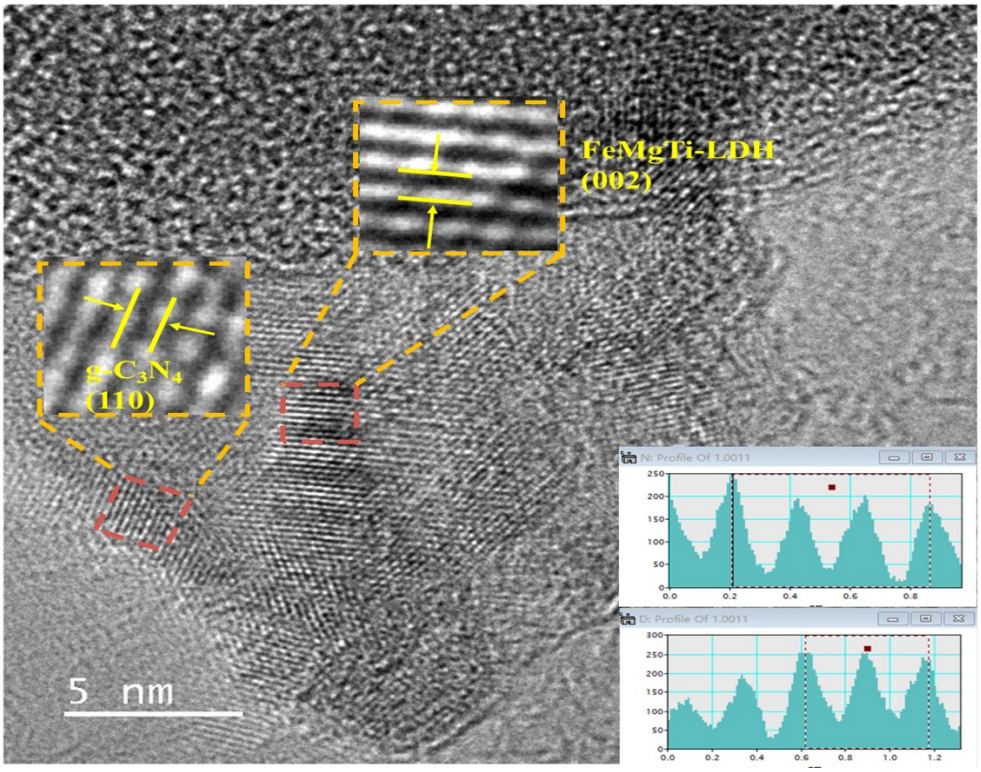

Fig. S3. the HRTEM image of MgFeTi (3:1)-LDH/g-C_3N_4

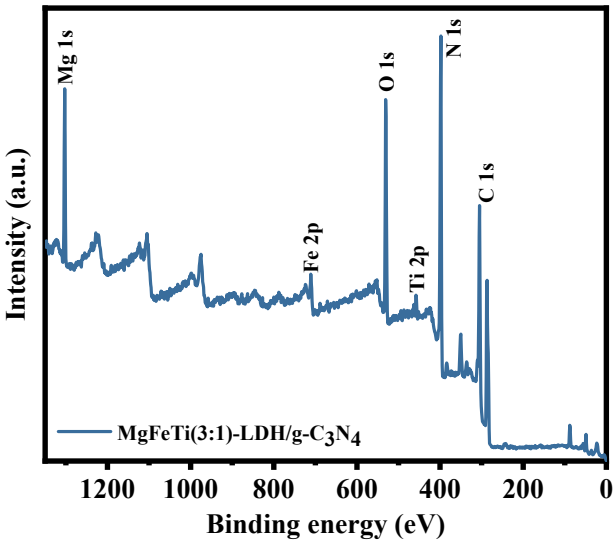

Fig. S4. XPS survey spectra of MgFeTi (3:1)-LDH/g-C_3N_4

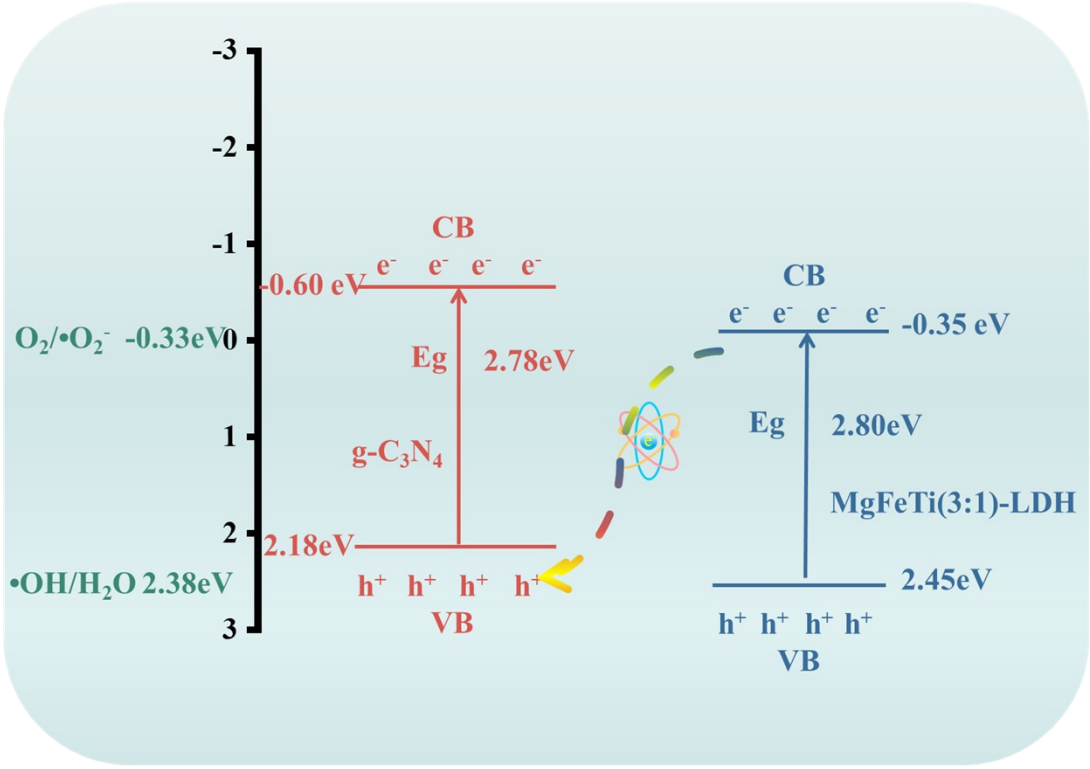

Fig. S5. CB and VB of the MgFeTi (3:1)-LDH/g-C_3N_4

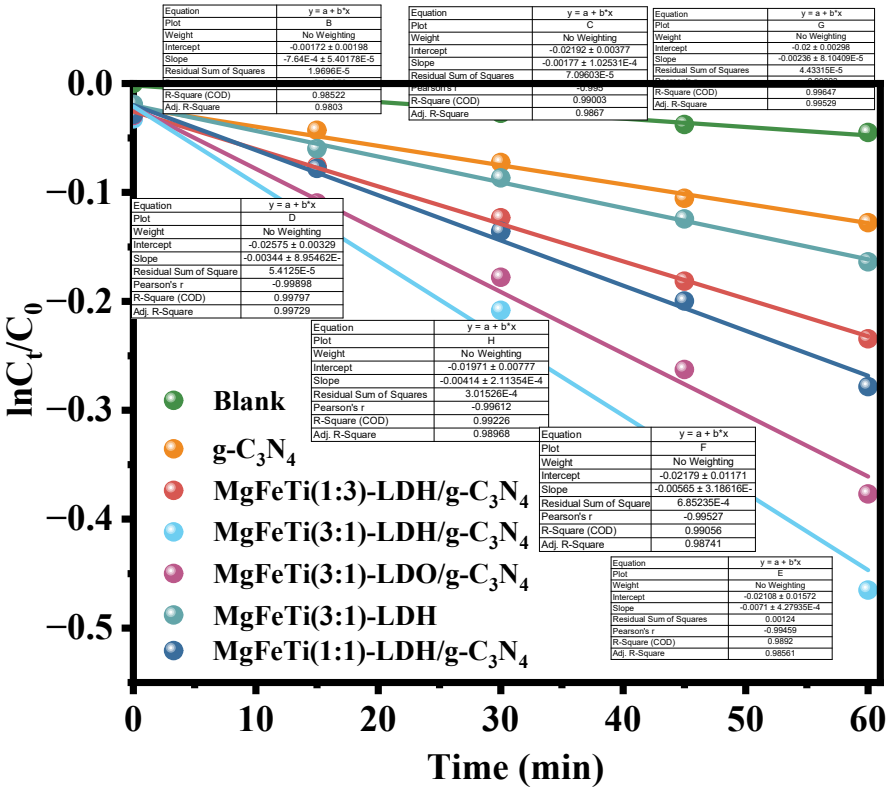

Fig. S6. kinetics of degradation reaction

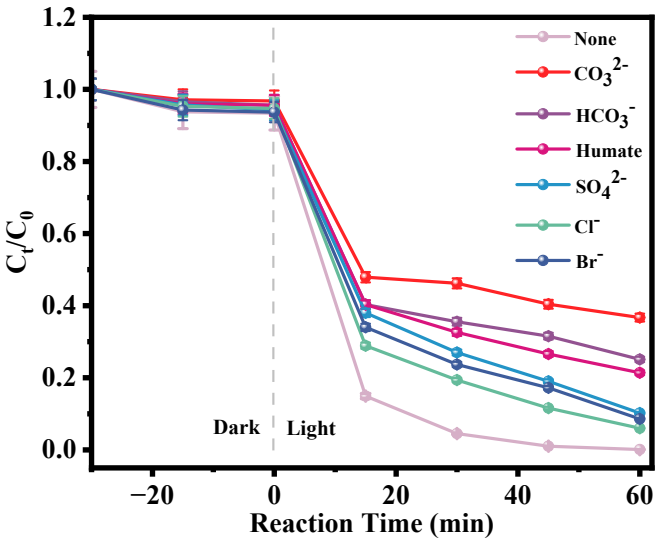

Fig. S7. The effect of various inorganic anions and humate on degradation efficiency

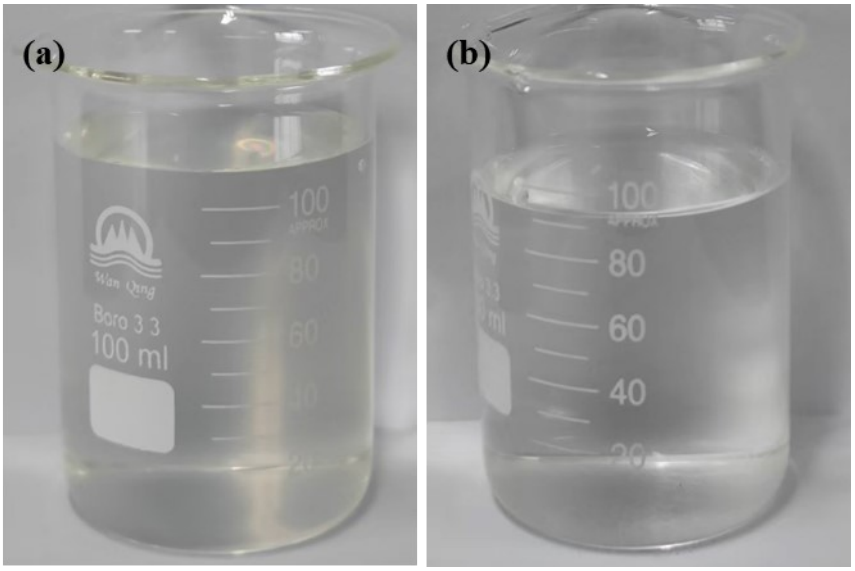

Fig.S8. The decolorization efficiency of MgFeTi-LDH/g-C_3N_4 composites for TCH in actual effluents (a) TCH in actual effluents, (b) Decolorized TCH solution

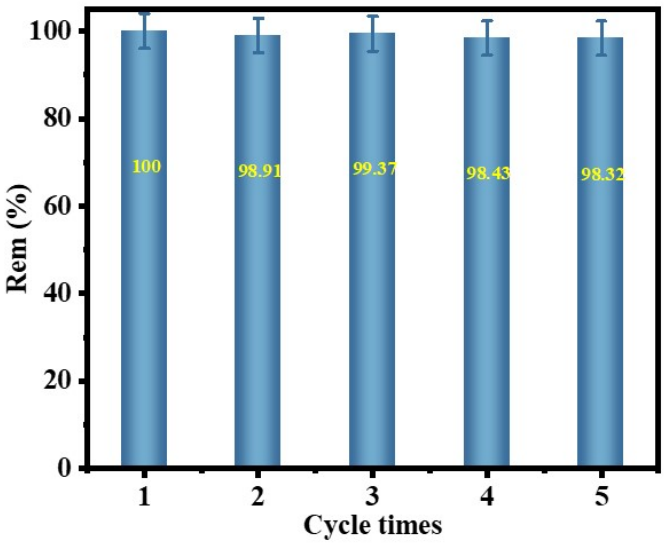

Fig. S9. Reusability performance of MgFeTi(3:1)-LDH/g-C_3N_4

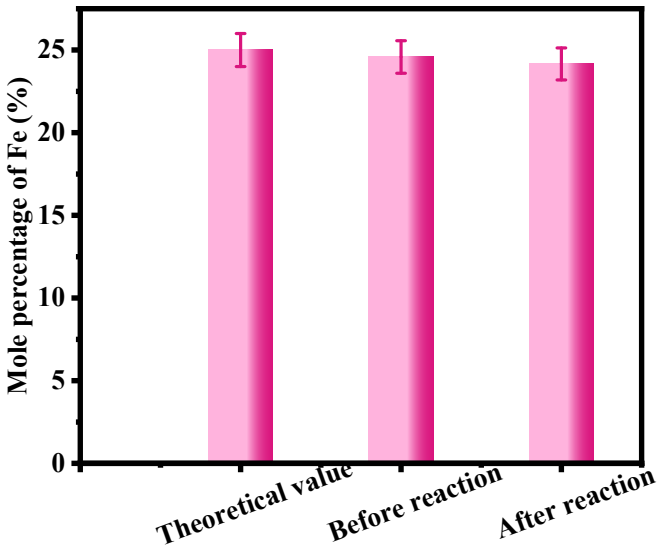

Fig. S10. The Fe mole percentage from ICP

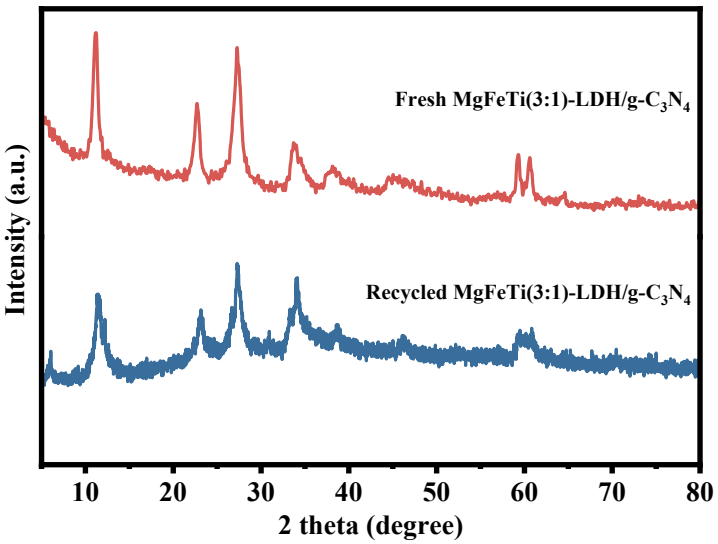

Fig. S11. The XRD patterns of recycled MgFeTi(3:1)-LDH/g-C_3N_4 and fresh MgFeTi(3:1)-LDH/g-C_3N_4

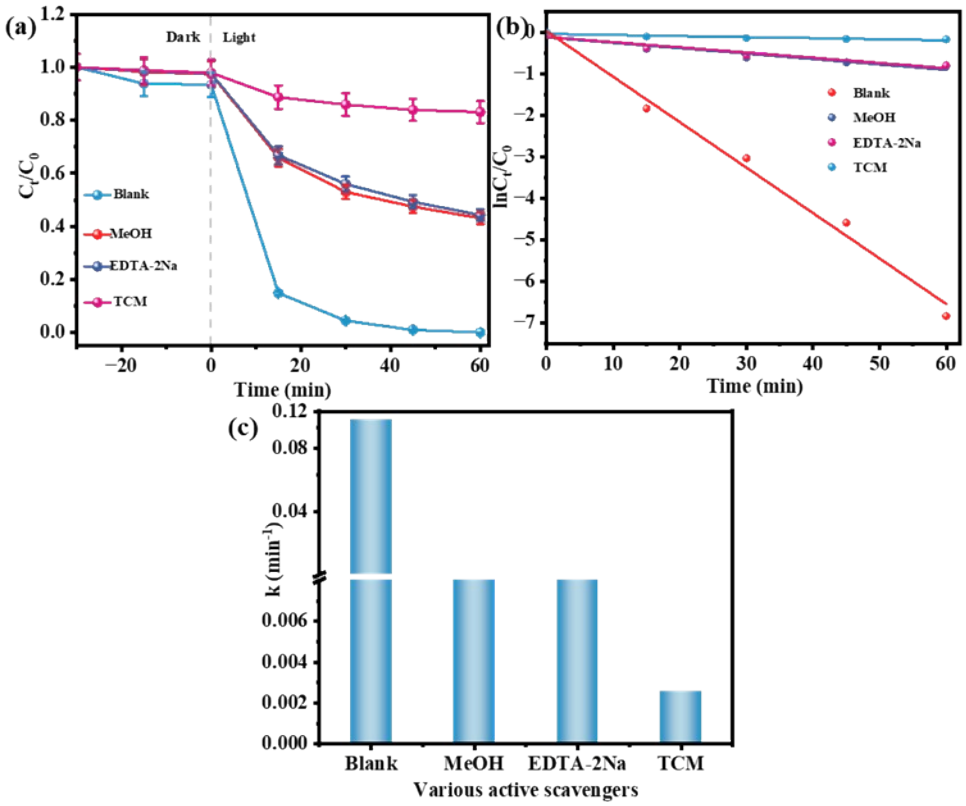

Fig. S12. The effects of various scavengers on (a) C_t/C_0, (b) $\ln C_t/C_0$, (c) k

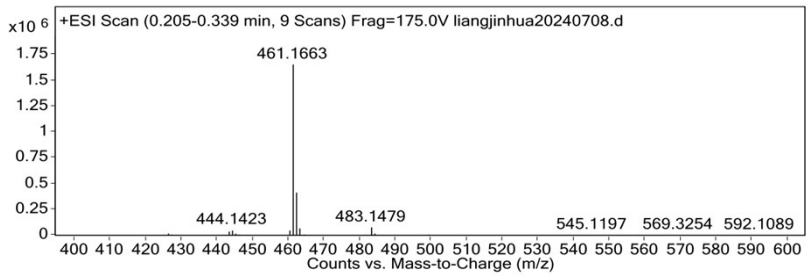

Peak List

m/z	z	Abund
426.1278	1	24250.21
443.1547		39067.73
444.1423		51209.78
445.1645	1	24314.13
460.1704		52432.11
461.1663	1	1656624.88
462.1695	1	419812.66
463.1715	1	74106.82
483.1479	1	75651.18
484.1508	1	18657.04

Fig.S13. LC-MS spectra of TCH photocatalytic degradation recorded by MgFeTi(3:1)-LDH/g-C_3N_4 at 0 min

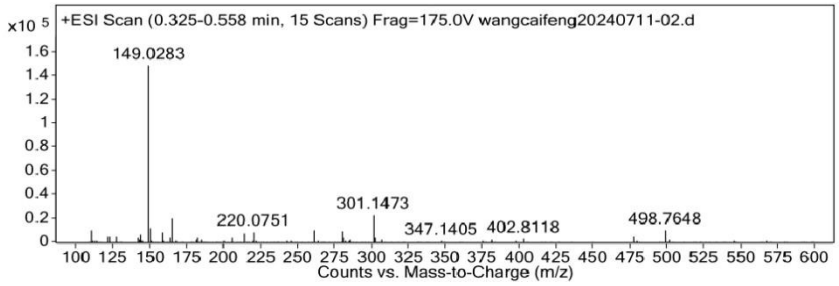

Peak List

m/z	z	Abund
110.0126	1	10526.15
149.0283	1	149214.95
150.0317	1	12777.19
158.159	1	9371.32
164.9255		20541.17
220.0751		8986.27
260.8784		10677.84
279.1652	1	9788.03
301.1473	1	23325.36
498.7648		10471.53

Fig. S14. LC-MS spectra of TCH photocatalytic degradation recorded by MgFeTi(3:1)-LDH/g-C_3N_4 at 30 min

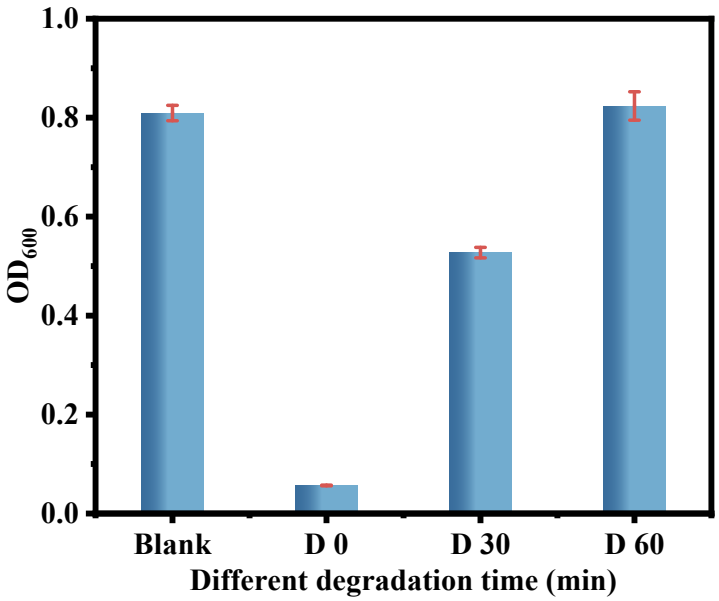

Fig. S15. Optical density (OD_{600}) values of degradation TCH at different time periods over MgFeTi (3:1)-LDH/g-C_3N_4